Absorption enhancement of silicon solar cell with Ag nanoparticles by surface plasmons resonance*

YUAN Zong-heng (袁纵横)[1,2]**, **LI Xiao-nan** (李骁男)[2], and **HUANG Jing** (黄静)[1]

1. School of Information Engineering, Guizhou Minzu University, Guiyang 550025, China

2. School of Electronic Engineering and Automation, Guilin University of Electronic Technology, Guilin 541004, China

(Received 7 September 2013)

The absorption enhancements of silicon layer in silicon solar cells with three kinds of Ag nanoparticles including sphere, cylinder and cuboid are studied by the finite difference time domain (FDTD) method, respectively. The results show that the light absorption of silicon is significantly improved due to the localized surface plasmon (LSP) resonance. The relations of the absorption enhancement with the parameters of nanoparticles are thoroughly analyzed. The optimal absorption enhancement can be achieved by adjusting the relevant parameters. Among the three types of Ag nanoparticles, i.e., sphere, cylinder and cuboid, the silicon with the cubical Ag nanopaticles shows the most efficient absorption enhancement at optimal conditions, its maximum absorption enhancement factor is 1.35, and that with the spherical Ag nanopaticles gets the lowest absorption enhancement. The work is useful for the further theoretical study and design for the plasmonic thin-film solar cell.

Document code: A **Article ID:** 1673-1905(2013)06-0405-5

DOI 10.1007/s11801-013-3160-x

Now, some methods for improving the absorption and enhancing the efficiency of the thin film solar cell have been proposed[1-5]. Such as, surface texturing is used for enhancing light trapping[6,7], and silicon nanowire arrays are set as an antireflection film to reduce the surface reflection[8]. Another important way is to use the textured back reflector for enhancing light trapping[9-11]. But the solar cell with back reflector may suffer from the back surface recombination loss. In addition, a nanostructure deposited on the top surface of a solar cell is also used[12-16].

In this paper, three kinds of Ag nanoparticles, including sphere, cylinder and cuboid, are set on the silicon layer of silicon thin-film solar cells, respectively. The effects of the parameter of Ag nanoparticle and the period of the nanoparticle array on the absorption of the silicon are studied.

Fig.1 shows the three kinds of structures used in this paper. The spherical, cylindrical and cubical Ag nanopaticles are set on the surface of the silicon substrate with thickness of 500 nm, respectively. Ag is used as the metal material for its obvious localized surface plasmon (LSP) effects as well as low light absorption. Since the wide application of monocrystalline silicon solar cells, silicon is selected as the absorbing layer. The optical parameters of silicon and Ag are from Ref.[17]. In Fig.1, r represents the radius of spherical and cylindrical particles, h represents the height of cylindrical and cubical particles, L represents the side length of the base of the cubical particles, p is the period of the nanoparticle array, and t is the thickness of the silicon substrate.

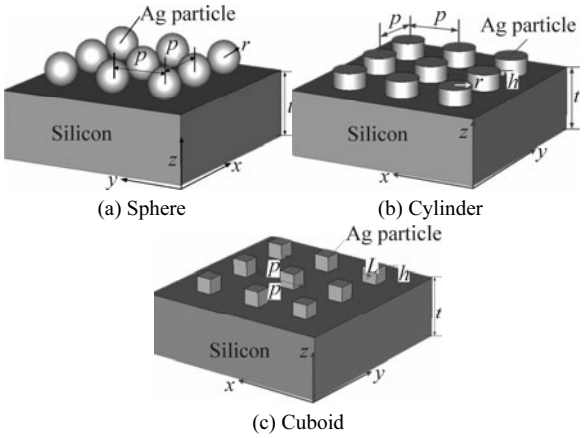

Fig.1 Solar cells with three kinds of Ag nanoparticles

The commercial software of Lumerical FDTD solutions is adopted for the numerical simulations. The incident source is a uniform plane wave with the wavelength range from 400 nm to 1100 nm, and the electric field is

* This work has been supported by the International Scientific and Technological Cooperation Projects of Guizhou Province in China (No.[2011]7035).

** E-mail:yuanzongheng@sina.com

polarized along *x*-axis. Perfectly matched layer (PML) absorbing boundary conditions are used on the upper and bottom boundaries of the computational domain which absorb the reflected and transmitted fields. Two power monitors are used for calculating the power absorbed in the silicon, one is located at the surface of the silicon, and another is located at the bottom. Thus, the absorbed power can be easily calculated by subtraction between them.

In order to estimate the efficiency of the solar cell, the quantum efficiency of $QE(\lambda)$ is defined as

$$QE(\lambda)=\frac{P_{\text{abs}}(\lambda)}{P_{\text{in}}(\lambda)}, \tag{1}$$

where $P_{\text{in}}(\lambda)$ and $P_{\text{abs}}(\lambda)$ are the incident light and absorbed light at the wavelength λ in the silicon solar cell, respectively. The integrated quantum efficiency of *IQE* is defined as

$$IQE=\frac{\int\frac{\lambda}{hc}QE(\lambda)I_{\text{AM1.5}}(\lambda)\text{d}\lambda}{\int\frac{\lambda}{hc}I_{\text{AM1.5}}(\lambda)\text{d}\lambda}, \tag{2}$$

where h is Plank constant, c is the speed of light in the free space, and $I_{\text{AM1.5}}$ is AM 1.5 solar spectrum. In Eq.(2), the numerator is equal to the number of photons absorbed by the solar cell, while the denominator means the number of photons falling onto the solar cell. The sun spectrum $I_{\text{AM1.5}}$ is taken from Ref.[18]. For estimating the improvement of the light absorption of the solar cell with metal particles, the absorption enhancement spectrum $g(\lambda)$ and absorption enhancement factor G are introduced and defined as

$$g(\lambda)=\frac{QE_{\text{particle}}(\lambda)}{QE_{\text{bare}}(\lambda)}=\frac{P_{\text{np}}(\lambda)}{P_{\text{bare}}(\lambda)}, \tag{3}$$

$$G=\frac{IQE_{\text{particle}}}{IQE_{\text{bare}}}=\frac{\int\lambda P_{\text{np}}(\lambda)I_{\text{AM1.5}}(\lambda)\text{d}\lambda}{\int\lambda P_{\text{bare}}(\lambda)I_{\text{AM1.5}}(\lambda)\text{d}\lambda}, \tag{4}$$

where $P_{\text{np}}(\lambda)$ and $P_{\text{bare}}(\lambda)$ represent the light absorption power values of silicon layer in the thin film solar cell with and without metal particles, respectively. IQE_{particle} and IQE_{bare} are the whole power values absorbed by the silicon with and without Ag nanoparticles, respectively.

Fig.2(a) shows the absorption spectra of silicon in solar cells with spherical Ag nanoparticles with different radii. It can be seen from Fig.2(a) that the wavelength position of the absorption peak and the peak value both change with radius. The largest peak value reaches 0.59 at the wavelength of 465 nm and the radius of 75 nm. Meanwhile, the absorption peak red-shifts when the radius is increased from 50 nm to 125 nm, while the absorption peak value is reduced after the first growth with radius from 50 nm to 75 nm. However, when r=200 nm, the light absorption is much lower than that of silicon without Ag nanoparticles (bare solar cell). It is because when the diameter of the sphere is equal to the period, Ag nanospheres are close to each other, which forms a reflective film, and a large amount of incident light is reflected back and another large portion is absorbed by Ag itself. It also can be found that the absorption ratio of the silicon thin film with spherical nanoparticles with radius from 50 nm to 125 nm is larger than that of bare silicon in a specific wavelength range. Fig.2(b) shows the absorption enhancement spectrum $g(\lambda)$ with different radii and fixed p and t, and there is a considerable absorption enhancement in near-infrared (NIR) region by the enhanced forward scattering due to the LSP resonance. It can be noted that $g(\lambda)$ is less than 1 when the wavelength is shorter than a specific wavelength (400–500 nm). For instance, when r=75 nm and the wavelength is shorter than 467 nm, the absorption of the silicon with nanoparticles is less than that of bare silicon. It can be explained in two ways. Firstly, Ag always has high absorption in this wavelength range due to the nature of the d-band absorption. Secondly, the absorption of silicon is proportional to the square of the electric field, and the total field in the silicon can be expressed as the superposition of the transmission field and the scattering field. When wavelength is below the plasmon resonance wavelength, a phase shift emerges between the transmission field and scattering field, so the absorption is less than that of the bare silicon substrate.

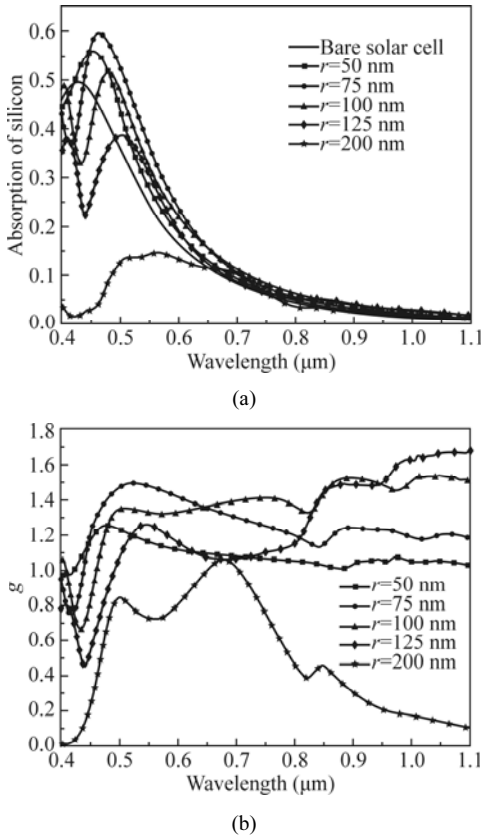

Fig.2 (a) The absorption spectra and (b) the absorption enhancement $g(\lambda)$ of silicon in solar cells with spherical Ag nanoparticles, where p=400 nm and t=500 nm

Fig.3 shows the relation of the absorption enhancement factor G and radius of spherical Ag nanosphere. It demonstrates that G increases with the increase of radius, until G reaches a maximum then begins to decrease gradually. The maximum G is 1.25 at r=75 nm.

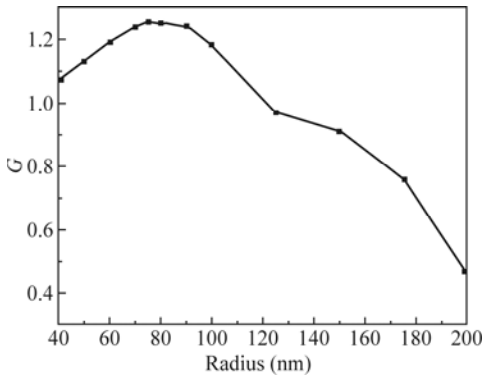

Fig.3 The relation of absorption enhancement factor *G* and radius of spherical Ag nanosphere when *p*=400 nm and *t*=500 nm

Fig.4(a) is the absorption spectra of silicon in solar cells with different periods of nanoparticle array. Fig.4(a) demonstrates that when period is 200 nm, the absorption is less than that of the bare silicon. Moreover, as the wavelength increases from 300 nm to 500 nm, the peak position red-shifts from 470 nm to 515 nm along with the fluctuation of the peak value, and this is similar to the case shown in Fig.2(a). As the wavelength increases from 300 nm to 500 nm, another peak appears, which leads to a larger optical absorption. When the period further increases till up to 800 nm, each nanoparticle acts as an isolated scatterer so that they have a little contribution to the absorption enhancement. It can be verified by Fig.4(b) that the enhancement factor G tends to 1 (no enhancement) with the further increase of period. The enhancement factor G takes the minimum when the period is equal to the diameter, strongly increases with period, until reaches a maximum, and then decreases to 1. Above discussions suggest that both radius and period have a significant impact on the absorption of the silicon in solar cell. The optimal G value is 1.276, at p=400 nm, r=75 nm and t=500 nm.

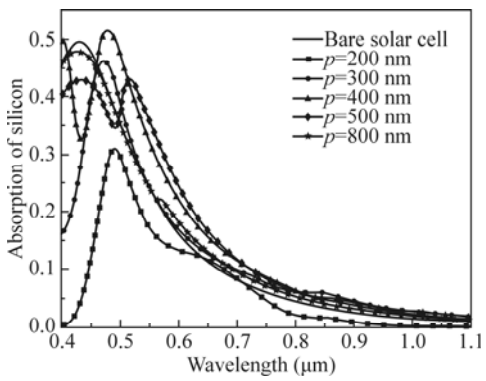

(a)

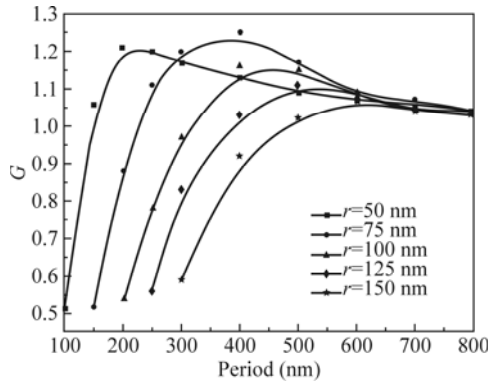

(b)

Fig.4 (a) Absorption spectra of silicon at different periods when *r*=100 nm and *t*=500 nm; (b) The relation of enhancement factor *G* with period at different radii of nanoparticles when *t*=500 nm

For the silicon with Ag cylinder and cuboid, the relations of absorption enhancement and period are similar to that with Ag sphere shown in Fig.4, and the effects of the diameter or side length and height of nanoparticles on the absorption enhancement are discussed.

Fig.5 is the curves of the relation between absorption enhancement factor G and the diameter of cylinder or the side length of cuboid at fixed p=300 nm, h=80 nm and t=500 nm.

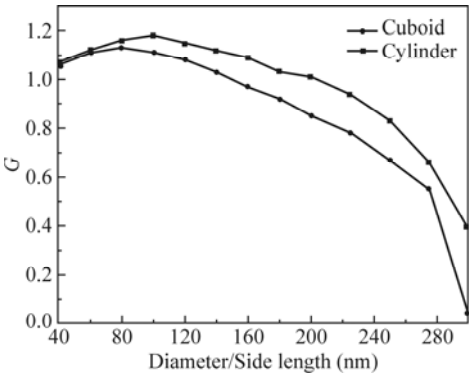

Fig.5 The relation of absorption enhancement factor *G* and diameter/side length at *p*=300 nm, *h*=80 nm and *t*=500 nm

The curves in Fig.5 are similar to that in Fig.3. G increases with the increase of diameter or side length, until G reaches a maximum, and then begins to decrease gradually. To cylinder, the G_{max} is 1.18 at diameter d=100 nm, and to cuboid, G_{max} is 1.13 at side length L=80 nm. It also shows that the silicon with Ag cylinder has greater G than that with Ag cuboid when p=300nm, h=80 nm and t=500 nm. This is because each particle array has its optimal period for absorption enhancement, and 300 nm is close to the optimal period of cylinder array.

Fig.6 shows the relation between absorption enhancement factor G and the height of the nanopaticle. It is shown that G fluctuates with the increase of the height,

and the reason is that as the height increases, the phase shift between the scattering field and the incident field changes periodically. In addition, the cuboid gets a higher G than the cylinder, and the cause is that 100 nm is close to the optimal period of cuboid. When the height increases to a value large enough, for example, h=800 nm, the absorption becomes lower than that of the bare silicon, i.e. G<1, and the cause is that the nanopaticles with larger height can weaken the transmission field greatly. In Fig.6, G_{max} is 1.35 for p=100 nm, L=44 nm and h=60 nm in this simulation of solar cell.

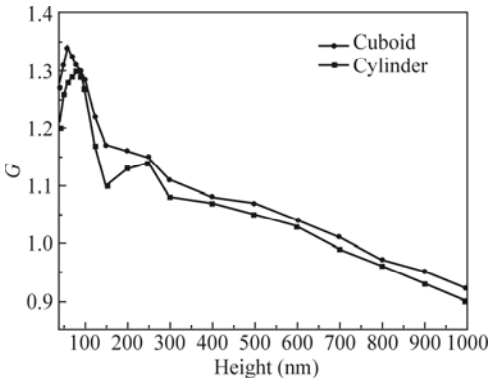

Fig.6 The relation between absorption enhancement factor *G* and height of the nanoparticle at *p*=100 nm, *d* or *L*=50 nm and *t*=500 nm

For comparing the effects of three kinds of nanoparticles, their absorption spectra and absorption enhancement spectra are depicted in Fig.7. Fig.7(a) shows the absorption spectra of silicon in solar cell with spherical, cylindrical and cubical Ag particles at optimal parameters. Fig.7(a) indicates that the solar cells with three kinds of Ag nanoparticles have more optical absorption compared with the silicon without Ag nanopaticle array. The absorption of silicon with spherical Ag nanoparticles is larger than that of silicon with cylindrical and cubical Ag particles in the visible light range. Conversely, the silicon with cylindrical and cubical nanoparticles has more efficient absorption in NIR range due to the LSP resonance. Fig.7(b) expresses the absorption enhancement spectra $g(\lambda)$ of the silicon with three kinds of Ag particles under their optimal case. The strongest enhancement g_{max} is g(520 nm)=1.49 for the silicon with spherical Ag particles, for cylindrical particles g_{max}= g(970 nm)=5.06, and for cubical particles g_{max}=g(1054 nm)=6.95.

In conclusion, the absorption enhancements of silicon layer in silicon solar cells with three kinds of Ag nanoparticles are investigated, respectively. The results demonstrate that the parameters of Ag nanoparticles can affect the absorption enhancement of silicon greatly. The absorption enhancement factor G rises as the period increases, until reaches the maximum, and then it begins to decrease. And the changes of G with radius, side length and height have the similar trend. The absorption enhancement peak can be tuned to the desired position of

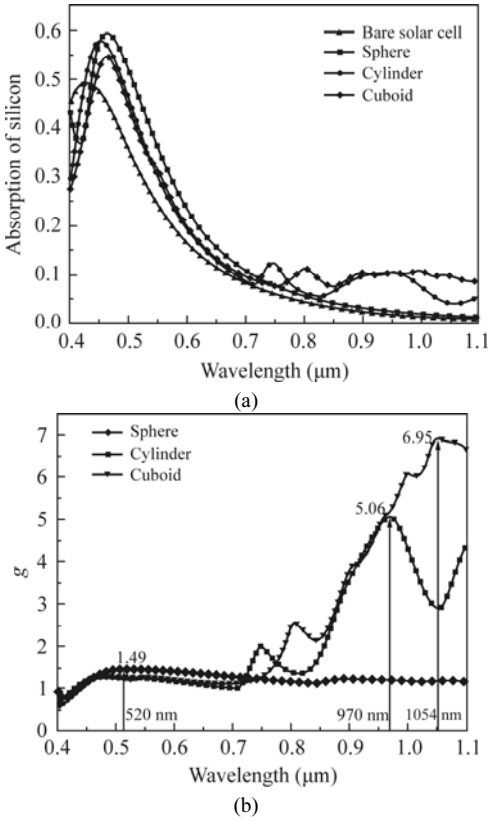

Fig.7 (a) Absorption spectra and (b) absorption enhancement spectra $g(\lambda)$ of silicon with three kinds of Ag nanoparticles under optimal parameters

solar spectrum by adjusting the appropriate parameters of Ag nanoparticle. The cubical Ag nanoparticles have greater enhancement role than spherical Ag particles and cylindrical particles, and the silicon with spherical Ag nanoparticle array has the lowest absorption enhancement among them. The trends of absorption enhancement with period, height and side length are convenient for finding the optimal parameters of Ag nanoparticle array and optimizing the design of plasmonic thin-film solar cell. The methods in this study can be followed to complete similar analyses of other structures. Furthermore, it should be noted that the results are not perfectly optimized due to the limited scope in our simulation. However, the work is useful for the further theoretical study and the optimization of the plasmonic thin-film solar cell.

References

[1] Rui Xu, Xiaodong Wang, Liang Song, Wen Liu, An Ji, Fuhua Yang and Jinmin Li, Opt. Express **20**, 5061 (2012).

[2] F. Cortés-Juan, C. Chaverri Ramos, J. P. Connolly, C. David, F. J. García de Abajo, J. Hurtado, V. D. Mihailetchi, S. Ponce-Alcántara and Guillermo Sánchez, Journal of Renewable and Sustainable Energy **5**, 033116 (2013).

[3] DING Guo-jing, QIN Wen-jing, YANG Li-ying, HUANG Kang and YIN Shou-gen, Journal of Optoelectronics·Laser **23**, 1786 (2012). (in Chinese)

[4] M. Y. Kuo, J. Y. Hsing, T. T. Chiu, C. N. Li, W. T. Kuo, T. S. Lay and M. H. Shih, Opt. Express **20**, A828 (2012).

[5] Chuanhao Li, Liangping Xia, Hongtao Gao, Ruiying Shi, Chen Sun, Haofei Shi and Chunlei Du, Opt. Express **20**, A589 (2012).

[6] Ping-Chen Tseng, Min-An Tsai, Peichen Yu and Hao-Chung Kuo, Progress in Photovoltaics: Research and Applications **20**, 135 (2012).

[7] Vladislav Jovanov, Ujwol Palanchoke, Philipp Magnus, Helmut Stiebig, Jürgen Hüpkes, Porponth Sichanugrist, Makoto Konagai, Samuel Wiesendanger, Carsten Rockstuhl and Dietmar Knipp, Opt. Express **21**, A595 (2013).

[8] LIN Xiao-yuan, HUANG Qian, ZHANG De-kun, MU Cun, ZHAO Ying, ZHANG Cun-shan and ZHANG Xiao-dan, Journal of Optoelectronics·Laser **24**, 523 (2012). (in Chinese)

[9] Wiesendanger S., Zilk M., Pertsch T., Rockstuhl C. and Lederer F., Opt. Express **21**, A450 (2013).

[10] Song B. S., Yamada S., Asano T. and Noda S., Opt. Express **19**, 11084 (2011).

[11] L. Zeng, Y. Yi, C. Hong, J. Liu, N. Feng, X. Duan, L. C. Kimerling and B. A. Alamariu, Appl. Phys. Lett. **89**, 111111 (2006).

[12] Fu-Ji Tsai, Jyh-Yang Wang, Jeng-Jie Huang, Yean-Woei Kiang and C. C. Yang, Opt. Express **18**, A207 (2010) .

[13] P. Spinelli, V. E. Ferry, J. van de Groep, M. van Lare, M. A. Verschuuren, R. E. I. Schropp, H. A. Atwater and A. Polman, Journal of Optics **14**, 024002 (2012).

[14] Richard S. Kim, Jinfeng Zhu, Jeung Hun Park, Lu Li, Zhibin Yu, Huajun Shen, Mei Xue, Kang L. Wang, Gyechoon Park, Timothy J. Anderson and Qibing Pei, Opt. Express **20,** 12649 (2012).

[15] Gaige Zheng, Linhua Xu, Min Lai, Yunyun Chen, Yuzhu Liu and Xiangyin Li, Opt. Communications **285**, 2755 (2012).

[16] Jonathan A. Scholl, Ai Leen Koh and Jennifer A. Dionne, Nature **483**, 421 (2012).

[17] E. D. Palik, Handbook of Optical Constants of Solids, Boston: Academic Press, 1991.

[18] Reference Solar Spectral Irradiance: ASTM G-173, 2003, http://rredc.nrel.gov/solar/spectra/am1.5/ASTMG173/ASTMG173.html.